ASTRONOMICAL APPLICATIONS OF ECHELLE SPECTROSCOPY

⁂2089

Frederic H. Chaffee, Jr.
Smithsonian Institution, Mount Hopkins Observatory, Amado, Arizona 85640

Daniel J. Schroeder
Department of Physics and Astronomy, Beloit College, Beloit, Wisconsin 53511

During the past decade astronomers have begun to make extensive use of the echelle grating (hereafter called echelle) as a dispersing element in Cassegrain spectrographs. This development has been prompted by the availability of high-quality replicas made from masters ruled on interferometrically controlled ruling engines (Harrison & Thompson 1970). In this article we review the general characteristics of echelles and the astronomical applications for which echelle spectrographs have been used, with the emphasis on the latter. Our discussion of applications is limited to those for which an echelle spectrograph is used at the Cassegrain focus. We also consider briefly selected planned echelle instruments and intended applications.

REVIEW OF ECHELLE PROPERTIES

Distinctive Features

The term *echelle* denotes a diffraction grating specifically made to be used with large angles of incidence and diffraction and in high orders of interference. Under these conditions, an echelle has an angular dispersion that is several times larger (typically 5–10 times) than that of a conventionally used first- or second-order grating (Schroeder 1970). The effect of larger angular dispersion results in two noteworthy features: (*a*) plate factors normally associated with long-focal-length coudé cameras can be achieved in a Cassegrain instrument, thus eliminating the loss in efficiency of the mirrors needed to reach the coudé focus; and (*b*) for a given telescope and spectrograph collimator diameter an echelle instrument has larger throughput than a grating instrument at equivalent spectral resolving power (Schroeder 1970). Equations from which these statements are derived are given below.

As a consequence of working in high orders of interference, it is necessary to

use an auxiliary dispersing element "crossed" with the echelle to separate the various echelle orders. The resulting two-dimensional spectrum (called an echellogram) has a format ideally suited for projection onto a relatively small collecting area. This means that detectors with higher detective quantum efficiency (DQE) than photographic plates can be used to record large amounts of spectral data in a single exposure. The Mount Hopkins Observatory (MHO) Cassegrian echelle spectrograph, for example, has a plate factor of 1.6 Å mm^{-1} at λ4000, and 800 Å of spectrum can be recorded on a 40-mm circular format. Echelle instruments now in operation have been used with various image tube systems, Kron electronic cameras, and image dissector systems, as well as in the direct photographic mode.

Potential Disadvantages

Certain shortcomings, or at least potential problem areas, are also associated with echelles. Scattered light in the form of satellites and ghosts results from random and periodic ruling errors. Satellites are particularly serious when the echelle is used in the study of absorption spectra because such scattered light tends to fill in absorption lines, thus causing errors in such measures as equivalent line widths. With the newer ruling engines, however, such scattered-light problems appear to be well under control (Learner 1972, Harrison et al. 1972).

In the design of a Cassegrian echelle instrument, very careful attention must be paid to ensuring that the entire instrument is mechanically very rigid. This is true, of course, for any Cassegrain spectrograph, but is a point that cannot be overemphasized. For instruments with equivalent beam diameters, an echelle is generally several times more massive than a grating, thus requiring particular attention to the mounting of this critical element.

The two-dimensional format produced by the echelle/cross-disperser configuration can result in reduction problems. As seen in the displayed spectra in this paper, each order is tilted with respect to the direction of echelle dispersion, thus complicating microdensitometer scanning if analysis of large spectral ranges is required. Further details are given in a following section that discusses measurement of echelle plates.

Another feature of any echelle spectrum is the variation in intensity along a single order, an effect easily seen in an echellogram of any stellar spectrum. This change in echelle efficiency is determined by the effective width of an individual groove face, with the intensity distribution or blaze function ideally like that of a single slit. The variation of efficiency over short spectral intervals complicates data analysis for certain kinds of problems. In order to obtain accurate absorption-line profiles or emission-line intensities, it is necessary to compensate for this blaze function, a process that requires more data handling than otherwise might be necessary (Schroeder & Anderson 1971, Peterson & Title 1975).

GENERAL ECHELLE CHARACTERISTICS

We do not present here the complete theory of the echelle, but give only that basic information needed to understand the general features of echelles. For more

complete discussions the reader is referred to papers by Harrison (1949) and Schroeder (1967, 1970, 1974).

Angular Dispersion, Free Spectral Range, Plate Factor

Two views of an echelle section are shown in Figure 1, with a ray incident on the echelle at 0, the origin of the coordinate system for that ray. The angles α, β, and θ_B are the incidence, diffraction, and blaze angles, respectively, measured in the yz plane, and γ is the angle between the incident ray and the yz plane. In terms of these angles the diffraction equation is $m\lambda/\sigma = \cos\gamma\,(\sin\alpha + \sin\beta)$, where σ is the echelle groove spacing, and m is the order number for wavelength λ. From the

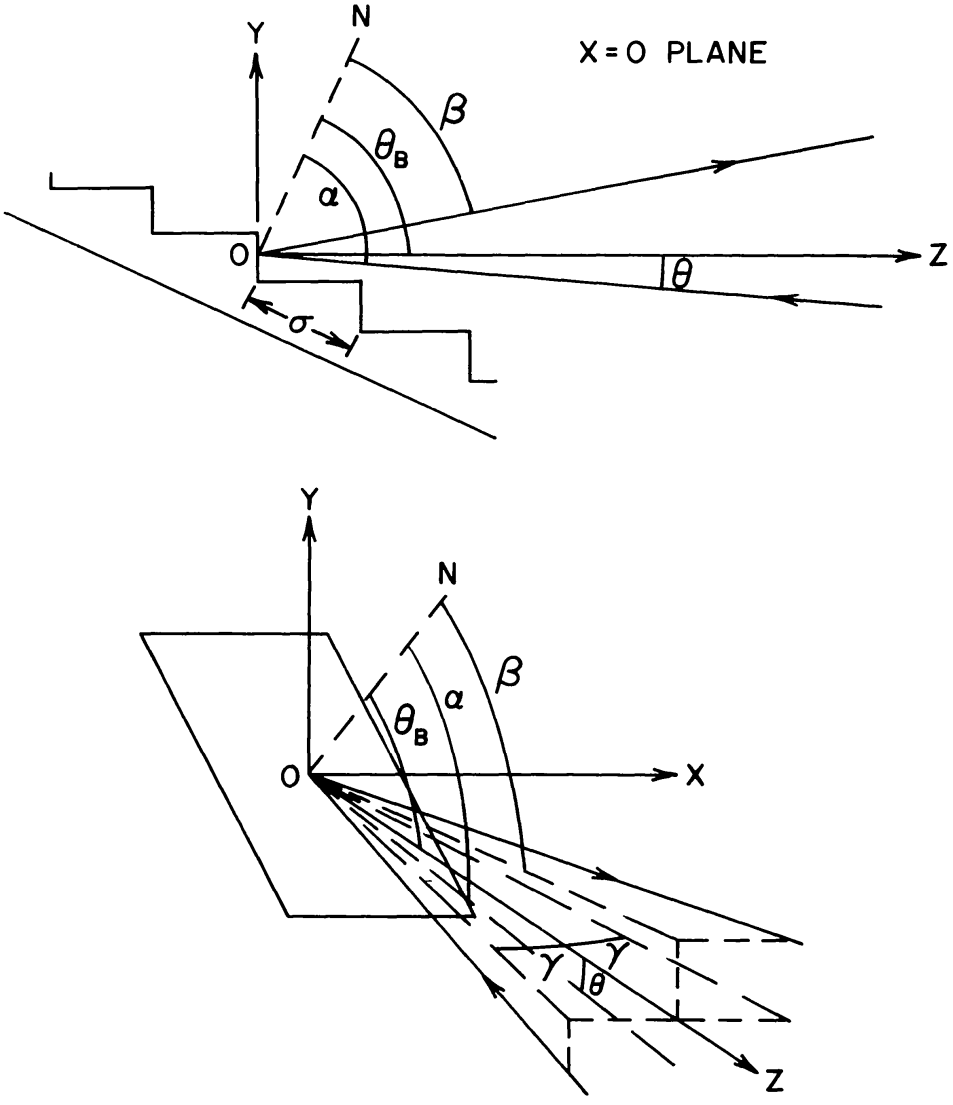

Figure 1 Local coordinate system for ray striking the echelle at 0, where the z axis is perpendicular to an echelle facet. 0N denotes the echelle normal. See text preceding Equation (1) for definitions of symbols. (Reprinted from Schroeder, D. J. 1970. *Publ. Astron. Soc. Pac.* 82:1253–75, Figure 1, with permission of the Editor.)

diffraction equation we find, for constant α and γ, that the angular dispersion is

$$d\beta/d\lambda = m/\sigma \cos\gamma \cos\beta = (\sin\alpha + \sin\beta)/\lambda \cos\beta. \quad (1)$$

If $\theta = 0$ and $\beta = \alpha = \theta_B$, then we find $d\beta/d\lambda = (2/\lambda) \tan\theta_B$, a relation that shows clearly that a large blaze angle means large angular dispersion. The most commonly used echelles have $\tan\theta_B = 2$, or $\theta_B = 63.5°$. For $\theta \neq 0$, we have $\alpha = \theta_B + \theta$, and $\beta = \theta_B - \theta$ at the blaze peak. The angular dispersion is less in this case, as compared with that for $\theta = 0$.

The free spectral range $\Delta\lambda$ is the wavelength difference between two wavelengths in successive orders at the same angle β, with $\Delta\lambda = \lambda/m$. If we choose β at the blaze peak, then we have

$$\Delta\lambda = \lambda^2/2\sigma \cos\gamma \cos\theta \sin\theta_B. \quad (2)$$

Every wavelength λ is found in one echelle order within $\Delta\lambda/2$ or less of the blaze wavelength for that order.

The plate factor, or reciprocal linear dispersion, is $P = (f_2 d\beta/d\lambda)^{-1} = \sigma \cos\gamma \cos\beta/mf_2$, where f_2 is the spectrograph camera focal length. If the spectrograph entrance slit width is w and the collimator focal length is f_1, then the projected slit width in the camera focal plane $w' = rw(f_2/f_1)$. The factor r in this expression is the anamorphic magnification of the dispersion element. The anamorphic magnification is simply the ratio of the collimator beam diameter and the diffracted beam width of a monochromatic source, the latter measured in the $x = 0$ plane of Figure 1. For an echelle or grating, we have $r = \cos\alpha/\cos\beta = |d\beta/d\alpha|$, a relation derived from the diffraction equation.

Spectral Resolving Power

In order to minimize w', it is clear that $r < 1$ is the appropriate choice, and hence $\alpha > \beta$. This choice is an important one because it results in greater spectral resolving power $\mathscr{R} = \lambda/\delta\lambda$, where $\delta\lambda$ is the spectral purity, the effective width of a monochromatic wavelength in the spectrograph focal plane.

The above statement is easily verified by evaluating the general expression for the spectral purity. By definition, we have $\delta\lambda = w'P = rw(f_2 d\beta/d\lambda)^{-1}$. Taking the expressions for w' and P from above and evaluating at the blaze peak give

$$\delta\lambda = \lambda w \cos\alpha/(2f_1 \sin\theta_B \cos\theta) \quad (3)$$

and

$$\mathscr{R} = 2f_1 \sin\theta_B \cos\theta/(w \cos\alpha). \quad (4)$$

Note that Equations (3) and (4) do not contain the angle β, but only α. Although the angular dispersion is smaller for $\theta > 0$ than for $\theta = 0$, the spectral resolving power is larger for $\theta > 0$ because of the anamorphic magnification. The effect is a significant one for an echelle where, for example, with $\theta_B = 63.5°$ and $\theta = 5.0°$, the spectral resolving power is about 1.2 times larger than for $\theta = 0$.

The range of resolving power for which an echelle instrument is particularly well suited for stellar observations can be easily determined. We assume the spectro-

graph is matched to the telescope, i.e. same focal ratios, in which case we have (Schroeder 1974)

$$\mathscr{R} = (d_1/D\psi) \cdot 2 \sin \theta_B \cos \theta/\cos \alpha, \tag{5}$$

where D = telescope diameter, ψ = angular width of entrance slit projected on the sky, and d_1 = collimator diameter. Taking typical angles as given, we find

$$\mathscr{R} = 10^4 d_1(\text{cm})/D(\text{m})\psi(''). \tag{6}$$

Assuming $\psi = 1''$ and taking as limits $5 \leqq d_1 \leqq 10$ cm, $1 \leqq D \leqq 5$ m, we find $\mathscr{R}$ in the range of 10^4 to 10^5. It is this range over which an echelle with $\tan \theta_B = 2$ is especially appropriate for stellar work, though, of course, larger $\mathscr{R}$s are possible if additional light loss at the entrance slit can be tolerated.

Blaze Function

It would appear advantageous from Equation (4) to increase $\mathscr{R}$ by choosing α, and hence θ, as large as possible for a given echelle blaze angle. This is not the case, however, because larger values of α significantly modify the blaze function and the distribution of light among wavelengths in different echelle orders.

If we take $\theta = 0$ and center the free spectral range on the blaze wavelength, then the echelle efficiency at each end of this range is slightly less than one-half that at the peak (Schroeder 1967, Davis 1970). The blaze wavelength itself is, of course, at the peak of the blaze function, and an ideal echelle with $\theta = 0$ will put all of the energy in this wavelength into this single direction. Other orders of the blaze wavelength will coincide with the minima of the blaze function. In this case the main peak of the blaze function covers two free spectral ranges.

When $\theta \neq 0$, the effective facet width is less than the actual width by a factor that depends on the groove shape and θ, and hence the angular width of the blaze function is increased. We also have smaller angular dispersion and thus each free spectral range occupies a smaller angular width. Assuming an ideal echelle with grooves having right-angle corners, we find that the number of free spectral ranges within the main peak of the blaze function is $2 \cos \beta/\cos \alpha$ (Schroeder 1970).

The effect of these two factors, broader blaze function and smaller angular dispersion, is to distribute the light of each wavelength more evenly between several echelle orders. For example, with $\theta = 10°$ (hence $\alpha - \beta = 20°$) and $\theta_B = 63.5°$, about 50% of the light of a blaze wavelength will be in the order at the blaze peak; most of the remaining light is in the two adjacent orders, one on either side of the blaze peak. Effectively, this is the same as reduced efficiency at the blaze peak. It is clear, therefore, that θ should be as small as is practical in order to have maximum efficiency.

Throughput

Given the high dispersion and resolving power of an echelle, it is worth comparing echelle and conventional grating instruments. This comparison is most conveniently made in terms of a quantity called the throughput, denoted here by $\mathscr{L}$. The monochromatic flux received in the spectrograph focal plane is directly proportional

to the spectrograph throughput (Jacquinot 1954, Meaburn 1970). In making this comparison, we assume a given telescope and similar seeing conditions so that only the spectrograph characteristics are relevant. We also assume for a stellar source that the entrance slit width is less than, or at most equal to, the seeing disk diameter. Denoting the echelle and grating instruments by e and g, respectively, we see that the comparison gives (Schroeder 1970)

$$\left(\frac{\mathscr{L}_e}{\mathscr{L}_g}\right)_{\mathscr{R}_e=\mathscr{R}_g} = \left(\frac{\mathscr{R}_e}{\mathscr{R}_g}\right)_{\mathscr{L}_e=\mathscr{L}_g} = \left(\frac{\tau_e}{\tau_g}\right)\left(\frac{r_g}{r_e}\right)\left(\frac{d_{ie}}{d_{ig}}\right)\frac{(d\beta/d\lambda)_e}{(d\beta/d\lambda)_g}, \tag{7}$$

where τ = spectrograph transmittance. When comparing a Cassegrain echelle instrument with a coudé grating, it is necessary to include in τ_g the efficiencies of the additional coudé mirrors. Because of the echelle's larger angular dispersion, the throughput advantage or resolving-power advantage of an echelle instrument can be significant.

Because transmitted flux, either integrated or monochromatic, is directly proportional to the throughput, it is essential to maximize this quantity. The required exposure time depends on detector characteristics. With photographic plates the speed depends on the area over which the flux/angstrom is distributed. With photon detectors the important parameter is the signal-to-noise ratio, and again the area over which the flux is distributed is important. For a noiseless detector, only the incident flux is important.

Cross-Dispersion Modes

There are various ways in which a cross-disperser can be incorporated into an echelle spectrograph (Schroeder 1970, 1974). The most practical arrangements for achieving broad spectral coverage have the cross-disperser somewhere between the collimator and camera optics. If the cross-disperser precedes the echelle in the optical train, it acts as a predisperser; if it follows the echelle, it is a postdisperser.

In the predisperser mode, the collimated light of different wavelengths strikes the echelle with different angles γ (see Figure 1), an arrangement that introduces spectral line tilt. For a given wavelength we can determine the change in β for changing γ, at constant α. The result is $d\beta/d\gamma = (\lambda\, d\beta/d\lambda)\tan\gamma$, where $d\beta/d\gamma$ is the tangent of the angle between a line parallel to the echelle rulings and a line along a focused spectral line. With γ as a function of wavelength in this mode, the orientation of spectral lines depends upon their location in the focal plane. This effect is generally undesirable, particularly if a broad spectral range is to be analyzed.

In the postdisperser mode all of the cross-dispersion is done on the diffracted beam from the echelle, and γ is constant for all wavelengths from the entrance slit center. Variable line tilt is then absent. The choice most often made for this mode is $\gamma = 0$. All of the displayed spectra in this paper were taken with spectrographs satisfying this condition, with a reflection grating as the cross-disperser.

Even in the postdisperser mode, γ will vary for each wavelength if a long, straight entrance slit is used. The relation above for $d\beta/d\gamma$ also applies in this case. The effect on a long spectral line in the focal plane is to introduce line curvature, with the radius of curvature $= f_2(\lambda\, d\beta/d\lambda)^{-1}$. Because of the echelle's larger angular dispersion, its lines are more strongly curved than those of a conventionally used grating.

A way to avoid this line curvature is to use a suitably curved entrance slit, though the difficulties of making such a slit would be formidable.

Having reviewed general echelle characteristics, we now consider the performance of existing echelle spectrographs in the measurement of radial velocities and in problems of line spectrophotometry.

RADIAL-VELOCITY DETERMINATIONS WITH ECHELLE SPECTROGRAPHS

Sources of External Error

Radial-velocity measurements with a Cassegrain echelle spectrograph are subject to all the errors traditionally associated with high-resolution astronomical spectroscopy.

Any differential motion among optical components in a Cassegrain spectrograph will produce an error in the measured radial velocity, which varies as the sum of sines and cosines of the zenith angle at which the observation was made. Thus the instrument rigidity requirements are severe if we wish to measure radial velocities to a precision comparable with those achieved in large coudé spectrographs of equivalent spectral resolution.

The Earth's atmosphere disperses light passing through it, and the magnitude of the dispersion increases with the tangent of the zenith angle. Depending on which part of the stellar image passes through the entrance slit, a wavelength shift can occur in the recorded spectrum. Because of the higher angular dispersion of an echelle, a larger fraction of the stellar image passes through the slit than for a coudé spectrograph at the same spectral resolution. Thus errors in radial-velocity measurements that arise from refraction effects will be larger for an echelle spectrograph (Petrie 1960).

A Cassegrain spectrograph is subject to changes in the ambient temperature, which are not experienced in a coudé spectrograph. Such changes in turn change the line spacing of the dispersive elements and the focus of the spectrograph. Either of these effects can produce shifts in the recorded spectrum and thus decrease the precision with which radial velocities can be measured.

Measurement of Echelle Plates for Radial Velocities

The reduction of an echellogram for radial velocities presents two unique problems.

1. Because two dispersive elements are used perpendicular to each other, the direction defined by the edges of the widened spectrum (usually referred to as the "dispersion direction" in single-grating spectrographs) is not parallel to the echelle dispersion. Thus, when the spectrum is aligned on a measuring engine with the spectrum edges parallel to the x axis, the direction defined by the slit jaws, which is perpendicular to the echelle dispersion, is tilted at an angle

$$\theta_{\text{slit}} = \arctan\left[(d\beta/d\lambda)_c/(d\beta/d\lambda)_e\right]$$

with respect to the y axis, where c and e refer to the cross-disperser and the echelle, respectively. For a typical echelle spectrograph we have $2.5° \leqq \theta_{\text{slit}} \leqq 6°$. As long as the measuring engine (or microdensitometer in the case of photometric reductions)

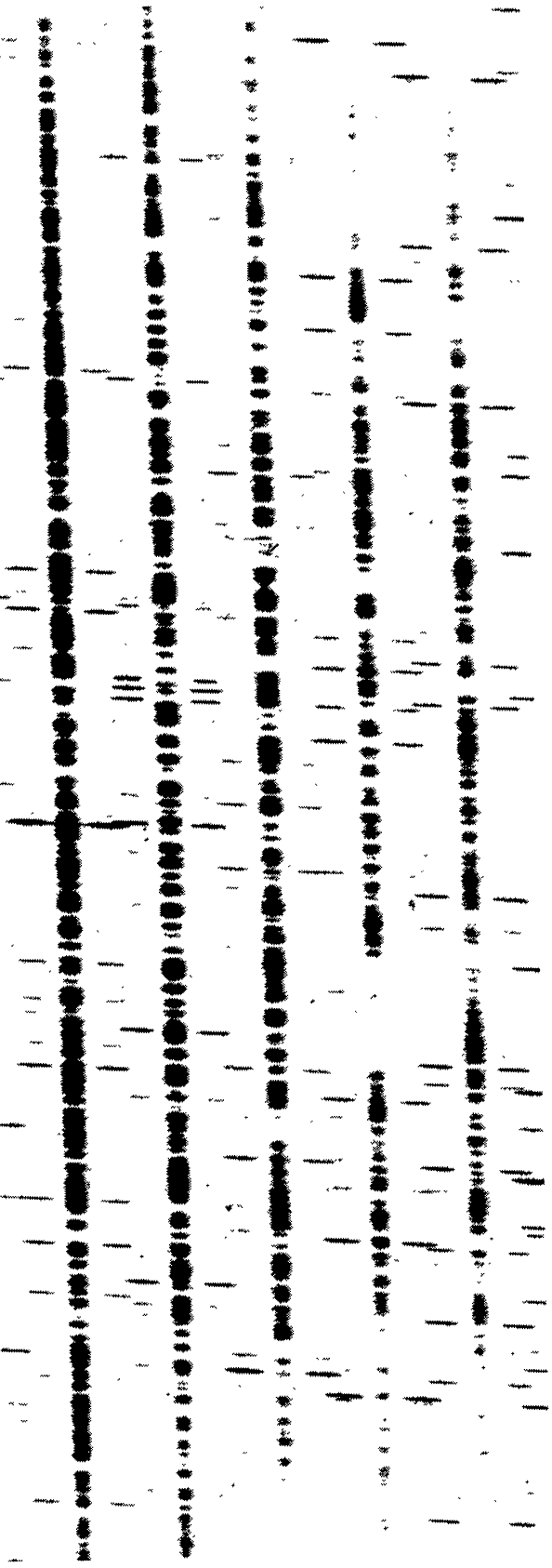

Figure 2 λ4300–λ4500 region of MHO echellogram EC-304 of α Boo used for radial-velocity measurement. Free spectral range = 35 Å; each order is 40-Å long; the strongest comparison line is λ4493.334; wavelength increases upward and to the right.

has a rotatable measuring slit that covers this range, reductions can be carried out just as they are for single-grating spectrograms.

2. A second-order dispersion solution must be generated for each echelle order in which stellar lines are to be measured for radial velocities. Because the free spectral range of an echelle order can be as small as 25 Å, a rich comparison source must be used to assure that enough comparison lines exist in each order to provide an adequate dispersion solution.

Sample Echelle Radial-Velocity Data

PHOTOGRAPHIC DATA To test the performance of an echelle spectrograph in measuring stellar radial velocities, we have obtained several high-resolution ($\mathscr{R} = 1.2 \times 10^5$) photographic echellograms for each of four IAU radial-velocity standards (Pearce 1955) using the MHO 1.5-m telescope and Cassegrain echelle spectrograph (Chaffee 1974).

Petrie & Fletcher (1967) have provided a line list to be used in measuring radial velocities of G and K stars and we have selected 18 of their 25 lines to be measured in the spectra of α Tau, β Gen, α Ari, and α Boo. These lines are located in echelle orders 126–130 and this spectral region is reproduced from plate EC-304 of α Boo in Figure 2. We have selected a Th-Ar hollow cathode lamp as sufficiently line-rich to provide adequate coverage for every echelle order in the range 3100 Å $\leqq \lambda \leqq$ 6500 Å. Wavelength identifications were taken from the thorium atlas of Breckinridge et al. (1975). Comparison lines were exposed above the spectrum prior to the stellar exposure and below it at the end of the exposure. The 3° tilt of the comparison lines relative to the normal to the edges of the stellar spectrum is seen clearly in Figure 2. The overlap of adjacent echelle orders of the comparison spectra results from the decision to minimize the cross-dispersion in order to maximize the spectral coverage when one uses the spectrograph with an image tube that has a limited detection area. This overlap increases toward the ultraviolet as the free spectral range decreases. Despite the resulting line blending of adjacent comparison orders, enough unblended Th-Ar lines remain to provide adequate spectral coverage down to the atmospheric limit.

The data for the radial-velocity plates are listed in Table 1. Plates for α Tau, β Gem, and α Ari cover a limited range of air mass, but were taken over several nights in order to examine the reproducibility of the results from night to night. The plates of α Boo were taken over a wide range of air masses in order to examine flexure and refraction effects on the resulting measured radial velocities. No strong correlation is seen between air mass and deduced radial velocity in Table 1. The data are summarized in Table 2 and compared with the IAU standard radial velocities for these stars. The agreement is excellent except for the case of β Gem, for which we have only three widely discrepant measurements. The quoted standard deviations are similar to those obtained from careful measurements of coudé plates at equivalent resolution (Petrie & Fletcher 1967).

IMAGE TUBE DATA As mentioned above, the output format of an echelle spectrograph renders it ideally suited for use with an image tube. All image tubes, however, are sensitive to changes in the magnetic field in their environment during the exposure,

Table 1 IAU radial-velocity standards measured with the MHO Cassegrain echelle spectrograph

Star	Plate no.	UT date	Hour angle at mid-exposure	Air mass	Exposure (minutes)	Heliocentric radial velocity (km sec^{-1})
α Tau	EC-282	28 Sept 74	−0:30	1.04	20	54.2
	EC-285	29 Sept 74	+0.29	1.04	20	53.8
	EC-287	30 Sept 74	+0.05	1.04	20	53.6
	EC-290	1 Oct 74	−0:04	1.04	20	54.0
β Gem	EC-283	28 Sept 74	−2:53	1.26	15	1.3
	EC-288	30 Sept 74	−2:23	1.17	15	2.1
	EC-291	1 Oct 74	−2:41	1.22	20	2.7
α Ari	EC-278	26 Sept 74	+1:17	1.06	45	−14.8
	EC-280	27 Sept 74	+0:52	1.03	45	−14.4
	EC-281	28 Sept 74	+0:37	1.02	45	−14.5
	EC-284	29 Sept 74	+1:56	1.12	45	−14.3
	EC-286	30 Sept 74	+1:14	1.05	45	−14.3
	EC-289	1 Oct 74	+1:02	1.04	45	−14.2
α Boo	EC-298	25 May 75	+5:29	3.50	10	−5.6
	EC-299	25 May 75	+5:52	4.82	10	−5.6
	EC-300	26 May 75	+0:24	1.03	10	−6.5
	EC-301	26 May 75	+3:18	1.44	7	−5.8
	EC-302	26 May 75	+4:29	2.06	8	−5.3
	EC-303	26 May 75	+5:00	2.60	8	−5.8
	EC-304	26 May 75	+5:21	3.19	10	−5.6
	EC-305	26 May 75	+5:43	4.20	10	−5.7

Table 2 Comparison of radial velocities measured with MHO echelle spectrograph with IAU standard heliocentric velocities

Star	MHO velocity	IAU standard velocity
α Tau	$+53.9 \pm 0.3$	$+54.1 \pm 0.1$
β Gem	$+2.0 \pm 0.7$	$+3.3 \pm 0.1$
α Ari	-14.4 ± 0.2	-14.3 ± 0.2
α Boo	-5.7 ± 0.3	-5.3 ± 0.1

and all introduce a certain amount of distortion into the image (Carruthers 1971). We would thus expect that radial velocities measured with any image tube cannot attain the high precision that we have reported from photographic plates.

A Kron electronic camera (Kron et al. 1969) has been used as the detector with the MHO echelle spectrograph on two problems requiring radial-velocity information. The MHO Kron camera produces a small amount of barrel distortion at the output. The magnitude of the distortion is about 6% of the radial distance from the center of the field.

Brown & Chaffee (1974) used 10 telluric-water-vapor lines for absolute wavelength calibration in their 6 July 1973 spectrum of the Na I D-line emission from Io. Even at relatively low resolving power ($\mathscr{R} = 3 \times 10^4$), the observed D-line radial velocity agrees to within 0.4 km sec^{-1} with that predicted from the orbital velocity of Io. Multiple measurements by this technique were not obtained because decreased humidity in subsequent observations eliminated the telluric-water-vapor lines as a wavelength calibration source.

When a laboratory comparison spectrum is required for wavelength calibration, image tube plates are slightly more complicated to reduce for radial velocities than photographic plates. Because of distortion, separate dispersion solutions must be computed for both the upper and lower comparison spectra. Each solution is then applied to the stellar spectrum, and the radial velocity is calculated by interpolation. This method of reduction was applied by Chaffee (1975) to determine interstellar-line radial velocities for four stars in Ophiuchus. In the interstellar-line spectrum of ζ Oph, he compares radial velocities deduced from echellograms with $\mathscr{R} = 1.2 \times 10^5$ with those measured by Hobbs (1973) with a PEPSIOS have $\mathscr{R} = 2.5 \times 10^5$. From three Kron camera plates, a mean velocity of -14.8 ± 0.3 km sec^{-1} was determined for the Ca II K line and -13.2 ± 0.2 km sec^{-1} was determined for the CH^+ (λ4232) line. These are to be compared with Hobbs's values of -14.4 km sec^{-1} and -12.6 km sec^{-1}, respectively.

We now compare the precision with which radial velocities are measured with an echelle spectrograph using a Kron camera and direct photographic plates. From a line-by-line analysis of the 8 photographic plates of α Boo quoted in Table 1, we find a mean standard deviation per line of 0.39 km sec^{-1}. From all Kron camera spectra of the stars in Ophiuchus (three spectra for each star), we find 0.84 km sec^{-1} There is some indication from the Kron camera data that the errors increase for longer exposures, but the number of plates is too small to make such a conclusion statistically meaningful.

On the basis of the available radial-velocity data we conclude that a Cassegrain echelle spectrograph can be used to measure radial velocities photographically to a precision equal to that obtained with a coudé spectrograph at the same resolution. Furthermore, with a Kron camera (and by implication, with any other adequately shielded image tube) the precision with which radial velocities can be measured is about a factor of two lower than that achieved photographically.

SPECTROPHOTOMETRIC MEASUREMENTS WITH ECHELLE SPECTROGRAPHS

Use of an Echelle Spectrometer As a Photoelectric Scanner

The Pine Bluff Observatory (PBO) echelle spectrometer (Schroeder & Anderson 1971) has been used primarily as a two-channel photoelectric scanner (McNall et al. 1972a) or as a 256-channel instrument using an image tube–image dissector scanner (IT-ID) (McNall et al. 1972b).

In the two-channel scanner, one channel monitors 4% of the light, which has been diverted from the main beam passing through the slit. This monitor serves as

an exposure meter and as a measure of the quality of the sky conditions. The second channel is the exit slit of the spectrometer. The gratings on the PBO instrument are attached to precision screws, which allow precise wavelength scanning under control of a PDP-8 computer. With the 91-cm telescope at PBO, Anderson (1974) has studied the Ca II λ8498 line profiles for 28 stars with $\mathscr{R} = 3 \times 10^4$. At this resolving power, 10^3 photoelectrons were counted at each of 21 points on the profile in 2^h of observing time for a star with $V = 3.0$ in 3″ seeing.

Bohuski et al. (1974) have measured the [O III] λ5007/λ4363 ratios in the Orion nebula, in NGC 6853, and in a number of planetary nebulae. This represents an unusual application of the spectrometer in that they used a resolving power of only 1.4×10^3. The high angular dispersion of the echelle allows the use of a wide entrance slit and still separates λ4363 from the Hg I λ4358 night skyline.

Except for investigations of nebulae whose images are nearly monochromatic, the use of a single-channel detector on an echelle spectrometer is a very inefficient application of the instrument. The IT-ID scanner has been developed for the PBO echelle spectrometer to increase its efficiency. Anderson (1972) applied this instrument to an investigation of the line profiles of He I λ5876 in 12 O stars. His data can be scaled to the same resolving power, integration time, and counted events for comparison to the single-channel case quoted above. We find that the line profile for a star with $V = 7.7$ can be observed under those conditions.

Use of Echelle Spectrographs with Two-Dimensional Detectors for One-Dimensional Spectrophotometry

The greatest efficiency is realized when a two-dimensional detector is used to record the output of an echelle spectrograph. The extraction of spectrophotometric information from an echellogram involves problems not encountered with coudé spectrograms:

1. The slit is not perpendicular to the edges of the widened spectrum.
2. A simple echelle spectrograph, of which the PBO and MHO spectrographs are examples, produces astigmatism that is perpendicular to the echelle dispersion. Astigmatism arises when either the collimator or the camera mirror is not used in the Littrow configuration; and in the confined volume available to a Cassegrain spectrograph, this departure from normal illumination may be a few degrees for both mirrors.

A monochromatic point source at the entrance slit typically projects to a $20\,\mu \times 300\,\mu$ image at the focal plane in simple echelle spectrographs. Thus a stellar image is held stationary on the slit during an exposure and the astigmatism provides the widening. The intensity across the spectrum rolls off at the edges and it is this variable intensity profile that complicates the microphotometry of echellograms.

3. If an image tube is used as the detector, its distortion can often be ignored in coudé spectrograms that are centered on the photocathode, but it must be compensated for in echellograms that fill the field of the image tube.

PHOTOGRAPHIC SPECTROPHOTOMETRY Chaffee (1974) carried out interstellar-line spectrophotometry for stars in the Perseus OB2 cloud using the MHO echelle with

Table 3 Comparison of MHO photographic equivalent widths (mÅ) with other determinations

Line	Star	W_{MHO}	W_{Ref}	Reference
3873.998	ζ Per	3.0	3.5	Field & Hitchcock (1966)
3874.608	ζ Per	10.3	10.9	Field & Hitchcock (1966)
4232.539	ζ Per	2	3.2	Hobbs (1973)
3933.664	ζ Per	54	50	Marschall & Hobbs (1972)
3933.664	ξ Per	117	108	Marschall & Hobbs (1972)
4232.539	ξ Per	27	25	Hobbs (1972)
3933.664	o Per	98	67	Marschall & Hobbs (1972)

baked IIIa-J plates. With $\mathscr{R} = 1.8 \times 10^5$, he reached a continuum density of 1.0 at λ4000 in a 15^m exposure of ζ Per ($B = 2.96$) on the 1.5-m telescope.

The data were processed on the Kitt Peak PDS microdensitometer. The software for the PDP-8 computer does not allow the table to be driven at a fixed angle with respect to the x axis, nor can the slit be rotated. To compensate for the astigmatism, a 16-μ square projected aperture was used to sample the spectra. A raster 2000 μ along the spectrum and 300 μ perpendicular to it was sampled centered on each interstellar line; each strip was converted to intensity via the appropriate characteristic curve and the strips were co-added to produce the intensity tracing from which equivalent widths were measured. Because no compensation for the 3° tilt of the slit is made in this reduction scheme, the resolving power is reduced to 1×10^5. The quality of the spectrophotometric data obtained with the MHO echelle spectrograph can be estimated by comparing Chaffee's photographic equivalent widths with those measured by others at the same or at higher resolution. This comparison is given in Table 3.

IMAGE TUBE SPECTROPHOTOMETRY We list briefly investigations that have been carried out using phosphor-output image tubes on echelle spectrographs. In all cases, either the measured phenomenon is variable or it has not been measured by other techniques. Thus, there is no independent basis on which to judge the quality of the photometric data, and we mention these studies for the sake of completeness.

Gull et al. (1974) used an ITT-4051 image tube as the detector on a stigmatic echelle spectrograph fed by an $f/8$ 25-cm telescope. This package was flown in an airplane and was used to search for the λ8200 H_2O band in the atmosphere of Venus. The echelle order covering this wavelength was imaged across the center of the 50-mm image tube, and with $\mathscr{R} = 4 \times 10^4$ an upper limit of 1.8 mÅ was established for the λ8176 line.

Wu (1972) used the PBO echelle spectrograph with a Carnegie image tube on the 91-cm telescope to study the $\lambda\lambda$5780 and 5790 diffuse interstellar bands in 66 stars with $\mathscr{R} = 2.6 \times 10^4$.

Gallagher & Anderson (1976) have used the PBO echelle with the Carnegie image tube on the Kitt Peak National Observatory (KPNO) 4^m telescope to examine

emission-line profiles of 4 lines in the spectrum of the post-nova HL Del ($m_{pg} = 12$). Exposure times ranged from 16 to 60 minutes with $\mathscr{R} = 2.5 \times 10^4$.

ELECTROGRAPHIC SPECTROPHOTOMETRY The MHO echelle spectrograph has been used most frequently with a Kron camera as the detector. The camera is an electrographic tube in which the photoelectrons are electrostatically focused onto a nuclear track emulsion inserted into the vacuum with the 40-mm photocathode. The resulting electrogram has the following desirable characteristics for photometric applications: (*a*) Its DQE is typically 13% at λ4300; (*b*) the measured plate density (D) is directly proportional to the incident photon flux to within 1% over a dynamic range of 500 ($0.01 \leqq D \leqq 5.0$); and (*c*) the nuclear track emulsion truly integrates the electron signal and exhibits no reciprocity failure.

Chaffee (1975) has applied the MHO echelle–Kron camera system to the study of interstellar lines. With $\mathscr{R} = 1.3 \times 10^5$, 1% signal to noise was achieved per resolution element (10^4 effective photoelectrons recorded) at λ4000 for ζ Oph ($B = 2.58$) in 6 minutes. Because it is necessary to scan the spectrum only in the immediate vicinity of each interstellar line, the distortion introduced by the image tube can be ignored and the plates reduced in the same manner as in the photographic case. Table 4 summarizes all interstellar-line measurements made at MHO with the echelle–Kron camera system for which other measurements at equivalent or higher resolution have been reported.

Measurement of single lines or of only a few lines is a restricted application of echelle spectroscopy in that only a small amount of the information recorded on the detector is required to achieve the scientific goals. When complete information is required, the problem of extracting the data becomes the major one in the process.

Peterson (1976) has applied the MHO echelle–Kron camera system to an investigation of the phenomenon of supermetallicity in field K giants, requiring the measurement of the equivalent widths of 250 absorption lines in each spectrum.

Table 4 Comparison of MHO electrographic equivalent widths (mÅ) with other determinations

Line	Star	W_{MHO}	W_{Ref}	Reference
4232.539	9 Cep	14	13	Hobbs (1973)
3933.668	λ Cep	215	210	Hobbs (1971)
4226.728	λ Cep	9	9.2	Hobbs (1971)
3933.668	ζ Oph	39	34.2	Herbig (1968)
			36	Hobbs (1973)
			34.8	Shulman et al. (1974)
3968.470	ζ Oph	22	21.3	Herbig (1968)
			20.6	Shulman et al. (1974)
4232.539	ζ Oph	22	27.4	Herbig (1968)
			19	Hobbs (1973)
			21	Tull et al. (1975)
4300.321	ζ Oph	20	20.5	Herbig (1968)

Peterson & Title (1975) have developed an automatic procedure for a PDS microdensitometer with a PDP 11/45 controlling computer to produce an intensity versus wavelength tracing for all spectral information recorded on a 40-mm circular detector. Their procedure retains the full resolution on the original plate because the PDS table is programmed to scan such that the edge of the sampling aperture remains parallel to the edge of the projected slit jaws. The nonuniform astigmatic widening is corrected for by scanning each order in small strips and co-adding as described above. Image tube distortion cannot be ignored in this case and the microdensitometer is programmed to follow the curvature of each echelle order.

Sections of the spectrum can be displayed on a CRT where final rectification is made for the stellar continuum and the equivalent widths of lines designated by the operator are calculated and displayed. The reductions, from initial setup to completed equivalent width determinations, involve sampling and processing 10^6 data points per spectrum and require 11 hours of combined PDS, PDP, and operator time.

J. B. Lester and D. W. Latham (personal communication) have developed an alternate technique for a David Mann microdensitometer and PDP-8 computer to reduce distorted, astigmatically widened echellograms. They scan with a slit tall enough to cover only the densest region of each order and apply an analytical correction to compensate for the measured nonuniform widening. The microdensitometer must still be programmed to follow curved echelle orders, but only one scan is required for each order. Inherent in their technique is a loss of a factor of approximately 1.4 in the signal-to-noise ratio in the resulting tracing, whereas Peterson's and Title's technique extracts all of the information from the plate. In effect, Lester and Latham sacrifice a factor of two in observing time for increased simplicity of data analysis.

Two-Dimensional Spectrophotometry

Echelle spectroscopy has been applied to only a few problems that require spatial as well as spectral information. With simple echelle spectrographs such as the MHO and PBO instruments, the spatial resolution in the direction perpendicular to the echelle dispersion is limited to about 3″ because of the astigmatism. In their absolute radiometric investigation of Io's sodium cloud, Brown et al. (1975) were somewhat limited in their ability to deduce the apparent emission rate because of the convolution of Io's seeing disk by instrumental astigmatism.

If high spatial resolution is required, a stigmatic spectrograph must be used and this complicates the design of the instrument. The Cassegrain echelle spectrograph for the Kitt Peak 4-m telescope (Gull 1974) is an instrument in which some of the potential throughput has been sacrificed in order to produce stigmatic images. The resolution is 25 μ at the image plane, which corresponds to 0.″25 at the Cassegrain focus of the 4-m telescope.

Figure 3 is the [O III] line at λ5007 in the planetary nebula NGC 2392 taken with the 4-m echelle in 0.″7 seeing. The complete echellogram contains several such images at the positions of other expected nebular lines. For scale, the strong comparison line is Fe I λ5012.072 and the plate factor on the original plate is

2.55 Å mm^{-1}. A 30″ tall slit was used and several orders of the continuous spectrum of the ninth magnitude central star can be seen. Figure 3 clearly shows the extremely complex velocity structure of NGC 2392.

Figure 4 is a multislit 4-m echellogram of M42 that samples the nebular spectrum simultaneously at six separate spatial positions. The strong line at the top is Balmer-α, to its right is [N II] λ6584 and to its left [N II] λ6548. In the left-center is λ5876 of He I, and the strong line at the lower right is [O III] λ5007. Such multislit echellograms contain a large amount of two-dimensional velocity information in each of several atomic constituents in the nebula, and a complete analysis of such data has not yet been completed. Figure 4 further illustrates the line curvature mentioned earlier, which results from the fact that a tall slit subtends a large angle at the echelle grating.

CONCLUSIONS

We have seen that for slit-limited spectroscopy an echelle spectrograph, because of the high angular dispersion of the echelle grating, can provide a significant increase in throughput when compared with that attainable with a conventional grating spectrograph at the same resolution. Furthermore, in slitless spectroscopy,

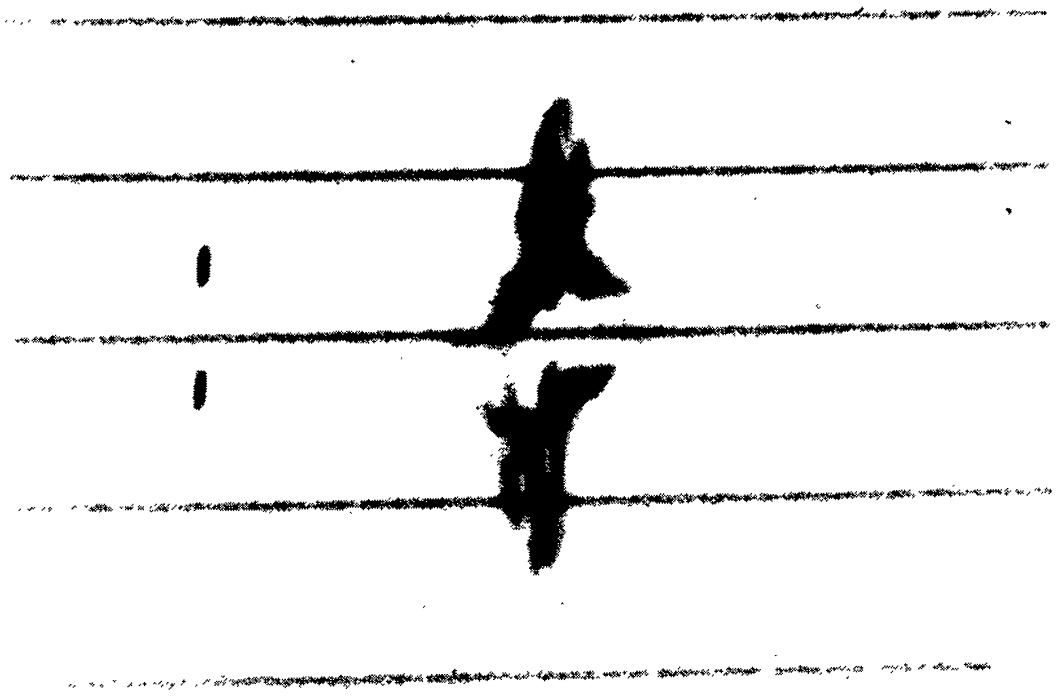

Figure 3 KPNO 4-m echellogram showing the λ5007 [O III] line in NGC 2392. (Courtesy T. R. Gull, Kitt Peak National Observatory.)

where no further throughput gain can be realized, a low-resolution echelle spectrograph still provides a convenient output format for data recording with any two-dimensional detector of limited size. Finally, the precision with which radial velocities and equivalent widths are determined with a Cassegrain echelle spectrograph is as high as that achieved with conventional coudé spectrographs.

We summarize in Table 5 the exposure times required to achieve 1% signal to noise in the continuum at $\mathscr{R} = 3 \times 10^4$ for the echelle spectrograph–telescope combinations shown. We have applied Latham's (1974) values for 103 type emulsions in order to convert from specular densities to equivalent photons for the 098-02

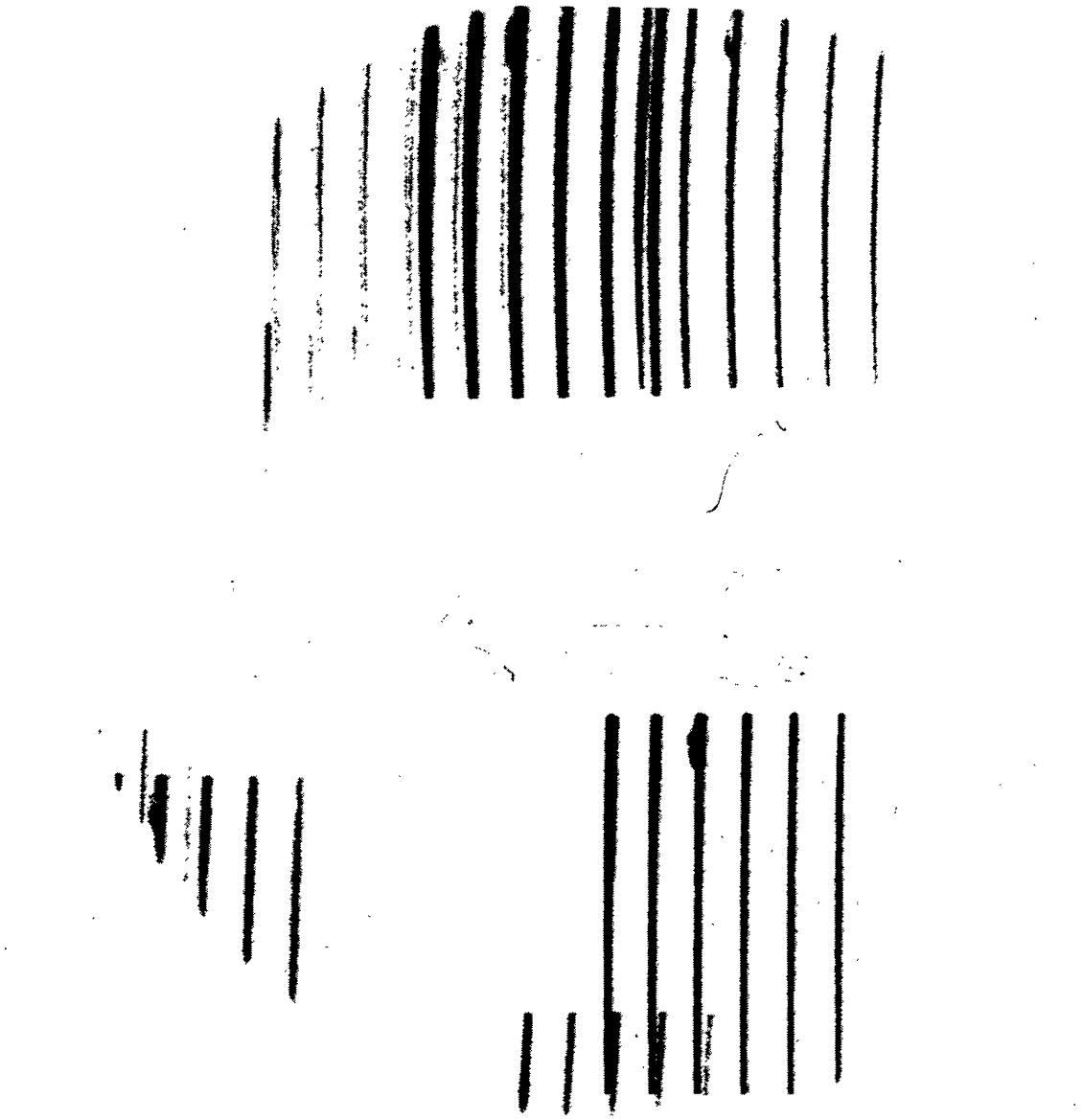

Figure 4 KPNO 4-m multislit echellogram of M42. See text for explanation. (Courtesy T. R. Gull, Kitt Peak National Observatory.)

Table 5 Comparative exposure times for echelle spectrograph–telescope systems ($V = 5.0$, $\mathscr{R} = 3 \times 10^4$, 10^4 equivalent photons per resolution element)

Telescope	Detector	Wavelength (Å)	Exposure (minutes)
0.9 m PBO	Single channel	8500	360
0.9 m PBO	IT-ID scanner	5900	95
1.5 m MHO	Kron camera	4000	13
1.5 m MHO	098-02 plates	5900	250
4.0 m KPNO	098-02 plates	5900	142

emulsion. The photographic estimates are scaled from short exposures and contain no correction for reciprocity failure. If the quantum efficiency of the detectors were the same, we would expect the PBO exposure times for the IT-ID scanner to be only a factor of two longer than those at MHO (the difference arising from the different telescope diameters and the extra reflection in the PBO spectrograph). Much of the remaining factor of 3.6 must result from the difference in seeing between the two sites.

A large percentage of our discussion has involved the rather complex techniques required to extract information from echelle spectrographs. It is important to summarize the sources of these difficulties and to outline the compromises that can be made to reduce them.

When an echelle spectrograph is used photographically, we have seen that radial-velocity information is extracted similarly to the way it is for coudé spectrograms, provided the measuring machine has a rotatable slit. Thus, the amount of measuring time is the same for the two instruments and the full throughput advantage of the echelle is realized.

Photographic spectrophotometry is somewhat more complicated with echellograms than with coudé spectrograms in that each echelle order must be scanned separately and the set-up time on the microdensitometer will be correspondingly longer. In addition, to extract all of the information from an astigmatic echellogram requires strip scanning and, thus, almost by necessity, a computer-controlled microdensitometer. Two compromises are possible to eliminate this complication: (*a*) A stigmatic spectrograph can be designed at the cost of increased complexity and with the probable loss of a factor of two in throughput because of the additional optical surfaces required; and (*b*) the echellogram can be traced with a single tall slit with the subsequent loss of a factor of approximately 1.4 in the resulting signal to noise compared with strip scanning each order, but with a large simplification of the reduction process.

A significant increase in complexity occurs when any detector is used that introduces distortion into the image. While radial velocities can still be measured from such plates with traditional measuring engines, the extraction of photometric information requires a computer-controlled microdensitometer system and a significant amount of software development. The method developed by Peterson and Title (which required 1.5 man years to complete) is an example of the approach required to extract all of the information from such plates.

If plates are bypassed as the detection medium and digital information is collected directly from the echelle spectrograph as at PBO, a computer must be an integral part of the system. Furthermore, if all of the available information is digitized with a large multielement digital detector, the storage and subsequent processing of 3×10^6 data points will be required, which involves the time-consuming development of computer software or image-processing systems.

For the observatory wishing to carry out traditional investigations in high-resolution spectroscopy, a simple echelle spectrograph can be built whose throughput is a factor of five higher than, and which achieves the same precision in radial velocity and spectrophotometric information as, a coudé spectrograph with optics of the same size. A minimum investment in modifying existing measuring engines to allow the slit to be rotated will permit the extraction of information from echellograms with the same ease (or difficulty) with which it is now taken from coudé plates.

For the observatory wishing to push instruments to the limit, a substantial investment in money and time is required to develop detector and data analysis systems (microdensitometer software and image processors). Such systems are often developed as part of the overall observatory effort and thus need only be modified for use with an echelle spectrograph.

Finally we should mention other promising echelle instruments that have only recently been developed. D. Bardas (personal communication) has constructed a prism predispersed echelle spectrograph that uses an echelle with $\theta_B = 28°$ to produce $P = 12.5$ Å mm^{-1} at $\lambda 6600$. The problem of variable line tilts discussed earlier for predispersed echelles is not as significant in this instrument because of the lower angular dispersion of the echelle. This instrument is used with an entrance slit that transmits all of the seeing disk and thus sacrifices no throughput because of its lower angular dispersion. It is to be used at moderate resolution ($\mathscr{R} = 6 \times 10^3$) for spectroscopy of faint sources. If the detector used is noise limited, this spectrograph should have a gain of four in output signal to noise compared with the other echelle spectrographs we have described because of the smaller area occupied by a resolution element on the detector.

Carswell et al. (1975) have developed an instrument that can best be described as intermediate between an ordinary Cassegrain spectrograph and an echelle. In their "echellette" spectrograph a 180-g-mm^{-1} grating, blazed at 4.5 μ, is used in the fifth through the thirteenth orders, postdispersed with a prism, to produce an echellogram with 33.7 Å mm$^{-1} \leqq P \leqq$ 87.4 Å mm^{-1} in the range 3230 Å $\leqq \lambda \leqq$ 8450 Å. With $\mathscr{R} = 2 \times 10^3$, they have obtained a spectra of the 16.6 magnitude quasar 1331 + 170 in 75^m on the Steward Observatory 2.3-m telescope.

These two spectrographs are designed to be used essentially slitless and hence use an echelle-like grating primarily to produce a convenient format and to achieve an intermediate plate factor for spectroscopy of faint sources.

ACKNOWLEDGMENTS

We wish to thank D. W. Latham, C. M. Anderson, R. C. Peterson, and A. M. Title for helpful discussions and suggestions, and D. W. Willmarth for assistance in radial-velocity reductions.

Literature Cited

Anderson, C. M. 1972. *Ap. J.* 190:585–90
Anderson, C. M. 1974. *Ap. J.* 177:L121–24
Bohuski, T. J., Dufour, R. J., Osterbrock, D. E. 1974. *Ap. J.* 188:529–32
Breckinridge, J. B., Pierce, A. K., Stoll, C. P. 1975. *Ap. J. Suppl.* 29:97–112
Brown, R. A., Chaffee, F. H. 1974. *Ap. J.* 187:L125–26
Brown, R. A., Goody, R. M., Murcray, F. J., Chaffee, F. H. 1975. *Ap. J.* 200:L49–53
Carruthers, G. 1971. *Astrophys. Space Sci.* 14:332–77
Carswell, R. F., Hilliard, R. L., Strittmatter, P. A., Taylor, D. J., Weymann, R. J. 1975. *Ap. J.* 196:351–61
Chaffee, F. H. 1974. *Ap. J.* 189:427–40
Chaffee, F. H. 1975. *Ap. J.* 199:379–82
Davis, S. P. 1970. *Diffraction Grating Spectrographs.* New York: Holt, Rinehart & Winston
Field, G. B., Hitchcock, J. L. 1966. *Ap. J.* 146:1–6
Gallagher, J. S., Anderson, C. M. 1976. *Ap. J.* 203:626–35
Gull, T. R. 1974. *Q. Bull. Kitt Peak Natl. Obs.* Oct.–Dec. 1974:20–27
Gull, T. R., O'Dell, C. R., Parker, R. A. R. 1974. *Icarus* 21:213–18
Harrison, G. R. 1949. *J. Opt. Soc. Am.* 39:522–28
Harrison, G. R., Thompson, S. W. 1970. *J. Opt. Soc. Am.* 60:591–95
Harrison, G. R., Thompson, S. W., Kazukonis, J., Connell, J. R. 1972. *J. Opt. Soc. Am.* 62:751–56
Herbig, G. 1968. *Z. Astrophys.* 68:243–77
Hobbs, L. M. 1971. *Ap. J.* 170:L85–88
Hobbs, L. M. 1972. *Ap. J.* 175:L39–41
Hobbs, L. M. 1973. *Ap. J.* 181:79–93
Jacquinot, P. 1954. *J. Opt. Soc. Am.* 44:761–65
Kron, G. E., Ables, H. D., Hewitt, A. V. 1969. *Adv. Electron. Electron Phys.* 28A:1–17
Latham, D. W. 1974. *Methods of Experimental Physics.* Vol. 12, *Astrophysics Part A: Optical and Infrared,* ed. N. Carleton, pp. 221–35. New York: Academic
Learner, R. C. M. 1972. Notes on grating ruling, testing, and test equipment. *AURA Eng. Tech. Rep. No. 39*
Marschall, L. A., Hobbs, L. M. 1972. *Ap. J.* 173:43–62
McNall, J. F., Michalski, D. E., Miedaner, T. L. 1972a. *Publ. Astron. Soc. Pac.* 84:176–81
McNall, J. F., Michalski, D. E., Miedaner, T. L. 1972b. *Publ. Astron. Soc. Pac.* 84:145–48
Meaburn, J. 1970. *Astrophys. Space Sci.* 9:206–97
Pearce, J. A. 1955. *Trans. IAU* 9:442
Peterson, R. C. 1976. *Ap. J. Suppl.* 30:61–83
Peterson, R. C., Title, A. M. 1975. *Appl. Opt.* 14:25–27
Petrie, R. M. 1960. *Astronomical Techniques,* ed. W. A. Hiltner, pp. 63–82. Chicago: Univ. Chicago Press
Petrie, R. M., Fletcher, J. M. 1967. *IAU Symp.* 30:43–48
Schroeder, D. J. 1967. *Appl. Opt.* 6:1976–80
Schroeder, D. J. 1970. *Publ. Astron. Soc. Pac.* 82:1253–75
Schroeder, D. J. 1974. See Latham 1974, pp. 463–89
Schroeder, D. J., Anderson, C. M. 1971. *Publ. Astron. Soc. Pac.* 83:438–46
Shulman, S., Bortolot, V. S., Thaddeus, P. 1974. *Ap. J.* 193:97–102
Tull, R. G., Choisser, J. P., Snow, E. H. 1975. *Appl. Opt.* 14:1182–89
Wu, C. C. 1972. *Ap. J.* 178:681–99